

A Wearable Fiberless Optical Sensor for Continuous Monitoring of Cerebral Blood Flow in Mice

Chong Huang, Yutong Gu, Jing Chen, Ahmed A. Bahrani, Elie G. Abu Jawdeh,
Henrietta S. Bada, Kathryn Saatman, Guoqiang Yu*, and Lei Chen**

Abstract— Continuous and longitudinal monitoring of cerebral blood flow (CBF) in animal models provides information for studying the mechanisms and interventions of various cerebral diseases. Since anesthesia may affect brain hemodynamics, researchers have been seeking wearable devices for use in conscious animals. We present a wearable diffuse speckle contrast flowmeter (DSCF) probe for monitoring CBF variations in mice. The DSCF probe consists of a small low-power near-infrared laser diode as a point source and an ultra-small low-power CMOS camera as a 2D detector array, which can be affixed on a mouse head. The movement of red blood cells in brain cortex (i.e., CBF) produces spatial fluctuations of laser speckles, which are captured by the camera. The DSCF system was calibrated using tissue phantoms and validated in a human forearm and mouse brains for continuous monitoring of blood flow increases and decreases against the established technologies. Significant correlations were observed among these measurements ($R^2 \geq 0.80$, $p < 10^{-5}$). This small fiberless probe has the potential to be worn by a freely moving conscious mouse. Moreover, the flexible source-detector configuration allows for varied probing depths up to ~ 8 mm, which is sufficient for transcranially detecting CBF in the cortices of rodents and newborn infants.

Index Terms—Optical spectroscopy, Blood flow measurement, Brain, Implantable biomedical devices

I. INTRODUCTION

Cerebral blood flow (CBF) is tightly regulated to meet brain metabolic demand for supporting functional activities. Cerebral hyperemia (a higher CBF than normal) can raise intracranial pressure, which can compress and damage delicate brain tissue. On the other hand, cerebral ischemia (a lower CBF than normal) can directly result in the death of brain cells. It is critical to maintain proper CBF in patients who have life threatening conditions like cardiac arrest, stroke, cerebral edema, and traumatic brain injury (TBI). Thus, continuous monitoring of CBF variations provides crucial information for understanding pathological mechanisms and developing

medical interventions for a variety of neurological and cerebral diseases.

Rodents (mice and rats) have been helping scientists investigate human diseases for more than a century and still make up 95% of the animal models used in biomedical research today. While cerebral hemodynamic changes are usually captured on anesthetized rodents to avoid motion artifacts, the impact of anesthesia on CBF has been observed [1-3]. The anesthesia effect can last for several hours, even after the animal regains consciousness, thus affecting study outcomes. The ability to continuously and longitudinally monitor CBF variations in freely moving conscious animals presents a significant opportunity for studying their correlations with pathophysiological consequences [4].

There are very few noninvasive tools available for continuous assessment of CBF in rodents. Optical techniques based on dynamic light scattering are the most common methods for CBF measurements at microvasculature level including laser Doppler flowmetry (LDF) [5] and laser speckle contrast imaging (LSCI) [6, 7]. Both LDF and LSCI, however, have limited penetration depths (generally < 1 mm) into the tissue, which constrains their applications in animals with a thicker skull (e.g., rats). A more recently developed method, near-infrared (NIR) diffuse correlation spectroscopy (DCS), provides a noninvasive CBF measurement in relatively deeper brain tissues (up to ~ 15 mm depth) [8]. DCS uses coherent point-source illumination and single-photon-counting avalanche photodiode (APD) detection of *temporal fluctuations of laser speckles* to accommodate spectroscopic measurements of CBF variations [9-12]. DCS has been proven to be a valid assessment of CBF variations in brains of animals, children, and adults [8, 13-16]. Although effective, DCS utilizes large and expensive lasers and APDs, which cannot be directly placed on subject's head. Thus, rigid and fragile optical fibers are needed for source and detector couplings, which significantly constrain the subject movement.

Our group recently developed and validated a novel fiberless diffuse speckle contrast flowmeter (DSCF), which provides a simple, low-cost, fast, flexible, and compact alternative for continuous monitoring of blood flow variations in relative deep tissues (up to ~ 8 mm depth) [17, 18]. This penetration depth is generally sufficient for transcranially detecting CBF in the cortices of rodents and newborn infants through the intact scalp and skull. DSCF uses a small NIR laser diode as a point source and a bare CCD chip with no lens as a 2D detector array to rapidly quantify *spatial fluctuations of laser speckles* resulting from moving red blood cells (RBCs). What distinguishes CCD detection in DSCF [17, 18] from the APD detection in DCS is the transition from measurements of *temporal fluctuations*

The authors acknowledge funding support from National Institutes of Health (NIH, R21-HD091118, R21-AR062356, R21-AG046762, and COBRE #1P20GM121327), American Heart Association (AHA #16GRNT30820006 and #14SDG20480186) and National Science Foundation (NSF #1539068).

C. Huang, J. Chen, A. A. Bahrani, and G. Yu are with the Department of Biomedical Engineering, University of Kentucky, Lexington, KY 40506 USA (*G. Yu's e-mail: guoqiang.yu@uky.edu).

Y. Gu is with Department of Electrical Engineering, University of Southern California, Los Angeles, CA, 90089 USA

E. G. Abu Jawdeh and H. S. Bada are with Department of Pediatrics, College of Medicine, University of Kentucky, Lexington, KY 40536 USA

K. Saatman and L. Chen are with Department of Physiology, Spinal Cord and Brain Injury Research Center, University of Kentucky, Lexington, KY 40536 USA (**L. Chen's e-mail: lei.chen@uky.edu)

(hundreds of milliseconds) to *spatial fluctuations* (a few milliseconds) of laser speckles on the measured tissue surface. In addition to the improvement of sampling rate, thousands of parallel pixels/detectors provided by the small and inexpensive CCD chip significantly improve the sampling density and reduce the cost/dimension of the instrument. In contrast to DCS probes with rigid optical fiber bundles [8], the connections between the DSCF probe and a control unit (circuits and a laptop) are all soft electrical wires/cables, offering the potential to build and install a wearable or wireless probe/device for continuous cerebral monitoring in freely moving subjects. Measurements of large flow variations by the DSCF prototype were compared to standard DCS in tissue phantoms and human forearms. The results showed no significant bias with good limits of agreement among these measurements. A remaining challenge in our DSCF prototype was the accumulated heat generated by excessive power consumption of the CCD chip (2 W, CMLN-13S2M-CS, Point Grey) [17]. Although heat sinks and a fan were used to cool down the high-power CCD chip, adding these parts made the DSCF probe large and impossible to be installed on a small rodent head.

The goal of this study is to explore a wearable, fiberless, flexible and compact DSCF sensor with ignorable heat load for continuous monitoring of CBF variations in mice. This miniaturized DSCF sensor consists of a small low-power laser diode (10 mW, L780P010, Thorlabs) as a point source and an ultra-small low-power CMOS camera (4 mW, NanEye 2D, Awaiba) as a 2D detector array, which can be safely installed on a mouse head. In addition to this significant improvement, the circuit to drive the laser diode was re-designed to stabilize the output light intensity via utilizing a feedback circuit reading from a built-in detector photodiode. A user-friendly graphical interface was also developed to control the source and detector for data collection and analysis. The performance of this novel DSCF system was first evaluated using tissue-simulating phantoms with known optical properties. For *in vivo* validations, blood flow variations in a human forearm and mouse brains were concurrently measured by the DSCF and other standards including LDF and DCS.

II. METHODS

A. Diffuse Speckle Contrast Flowmeter (DSCF)

DSCF Instrument. The DSCF system configuration is shown in **Fig. 1a**. After comparing multiple cameras, an ultra-small low-power camera (NanEye 2D Black & White; Dimension: $1 \times 1 \text{ mm}^2$, Power: 4 mW; Awaiba) was selected as a 2D detector to provide a 250×250 pixel-array with a maximum frame rate of 55 Hz (**Fig. 1b**). A tiny optical lens with a focus length of less than 1 mm was integrated on top of the camera sensor chip (Dimension: $0.75 \times 0.75 \text{ mm}^2$). The NanEye camera can cover a field of view (FOV) ranging from 2×2 to $6 \times 6 \text{ mm}^2$ by varying its working distance from 1 to 5 mm. In this study, we used a working distance of ~ 3 mm. The camera was driven by the commercial control board (NanoUSB2.2, Awaiba) made by the same provider. A graphical interface was designed using Microsoft C# to control

the camera for data collection. A small low-power laser diode with a built-in monitor photodiode (L780P010; Dimension: $\text{\O}5.6 \text{ mm}$, Power: 10 mW, Wavelength: $\text{\@}780\text{nm}$; Thorlabs) was powered by a custom-designed circuit (**Fig. 1d**). Briefly, an internal monitor photodiode detected continuously the light generated by the laser diode and sent feedback current to the Arduino Uno board for stabilizing the output light intensity. Stability test results over a period of 5 minutes suggested that this feedback circuit greatly reduced light intensity variations from 8% to $<1\%$ (data are not shown). A user-friendly graphical interface was created using LabView (National Instruments) to control the circuit for the laser diode package.

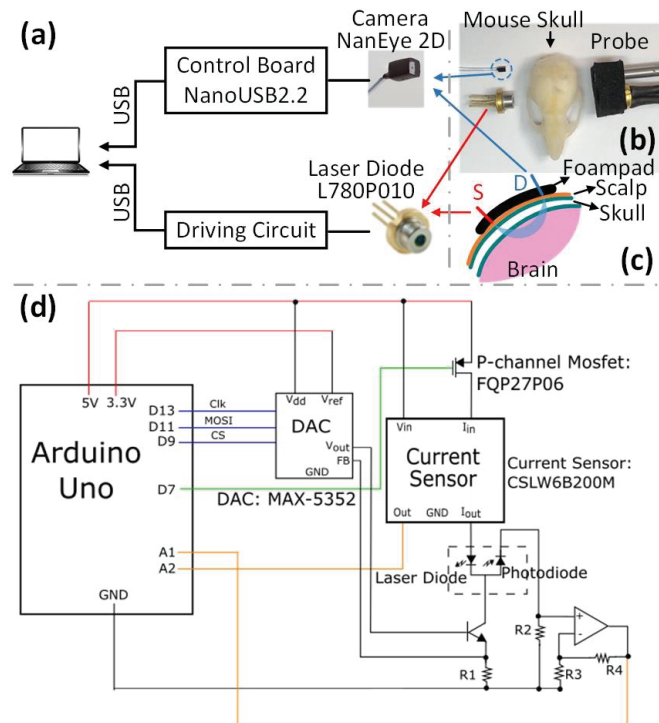


Figure 1: A DSCF system for CBF measurement. **(a)** A schematic diagram of DSCF device. **(b)** An ultra-small camera (NanEye 2D, Awaiba) and a small laser diode (L780P010, Thorlabs) confined by a black foam pad to create a DSCF probe. The tiny camera is protected by a 10-gauge needle. **(c)** A DSCF probe is placed on the top of a mouse head for CBF measurement. **(d)** A driving circuit with feedback current is used to actively stabilize the output power of the laser diode. D9, D11, and D13 pins of the Arduino Uno control the output of the digital-analog converter (DAC) via serial programmable interface (SPI). D7 connects to the gate of a P-channel mosfet to open and close the circuit. The A1 and A2 pins are used to read the analog voltages from the built-in photodiode and the current sensor (CSLW6B200M), respectively. These voltages are linearly proportional to the intensity of the light from and the current flowing to the gate of the bipolar junction transistor to control the current through the laser diode, effectively acting as a digital programmable current source.

Fiberless DSCF Probe. To make a DSCF probe, the tiny NanEye 2D camera was first wrap-sealed using a thin transparent film to avoid soaking damage from the liquid phantoms. The wrapped camera was then placed into a 10-gauge needle with a polished flat tip. The working distance between the NanEye 2D lens and the needle tip was ~ 3 mm to keep an appropriate focus. The laser diode and the camera needle were then confined by a black foam pad to build a DSCF probe to fix the source-detector (S-D) distance (**Fig. 1c**). Note that NIR light penetration depth in biological tissues is

approximately one half of the S-D distance [9-12]. The connections between the source/detector and a control unit (laptop) were all soft/flexible electrical wires and cables (i.e., fiberless).

DSCF Data Analysis. Details for DSCF data analysis can be found from our previous publication [17]. Briefly, NIR light generated by the laser diode diffuses through a “banana-shape” photon pathway inside a relatively deep tissue volume and reaches to the NanEye 2D camera (Fig. 1c). The movement of RBCs in the measured tissue volume produces continuous fluctuations of the laser speckles on the tissue surface, which are captured by the camera with a typical exposure time of 5 ms. The spatial speckle contrast (K) over a selected window of 7×7 pixels is determined by calculating the ratio of standard deviation (σ) and mean (μ) over these 49 pixels; i.e., $K = \sigma / \mu$. The dark and shot noise are first corrected with the method used in our previous studies [19, 20]. A blood flow index (BFI) is then extracted via a nonlinear relationship between the K and flow index under a semi-infinite geometry [17, 20, 21].

A sampling rate of 4 Hz was used for most of DSCF measurements. To increase the signal-to-noise ratio (SNR), a 3×3 adjacent pixel window with 9 values of K at the center of the sensor pixel array were averaged, representing one DSCF detector. Four adjacent frames of DSCF data were then averaged to align with the DCS data sampled at 1 Hz for comparison. However, to test DSCF measurements at a faster sampling of 20 Hz, a 6×6 adjacent pixel window array with 36 values of K were averaged, representing one detector for further SNR improvement.

B. Experimental Protocols

Characterization of DSCF Measurement Sensitivity and Stability Using Intralipid Liquid Phantom. The SNR of the DSCF measurement depends on the light intensity detected, which decays exponentially with the increase of S-D distance. The DSCF probe shown in Fig. 2a was designed for testing measurement sensitivity and stability at different S-D distances. The S-D distance varied from 10 to 30 mm with an interval of 2.5 mm via switching the detector tube to different locations. The probe was placed on the surface of a liquid phantom contained by an aquarium (dimensions: 200 mm \times 170 mm \times 60 mm). The liquid phantom, comprised of distilled water, India ink, and Intralipid, has been commonly used for the calibration of NIR measurement techniques [10, 19, 20]. India ink (Black India) was used to manipulate the absorption coefficient (μ_a) while Intralipid (Fresenius Kabi) provided particle Brownian motion (flow) and control of the reduced scattering coefficient (μ_s'). Optical properties of the liquid phantom were set as $\mu_a = 0.025 \text{ cm}^{-1}$ and $\mu_s' = 8 \text{ cm}^{-1}$ to mimic the biological tissue. DSCF measurements were performed continuously for 10 seconds at each S-D distance with a sampling rate of 4 Hz while the room light was turned off.

Concurrent DSCF and DCS Measurements of Intralipid Particle Flow Changes. A hybrid probe shown in Fig. 2b was designed for concurrent DSCF and DCS measurements of dynamic flow changes of Intralipid particles created by changing the phantom temperature. Increasing the temperature

results in an increased particle Brownian motion (flow) [17]. The temperature was initially set up to 45 °C by an immersed heater (CH103, Ovente), and then decreased naturally until reaching the room temperature of ~ 25 °C. A thermometer sensor (Physitemp) was placed inside the liquid tissue phantom for temperature monitoring. For DCS measurement, a long-coherent laser (DL785-100, CrystalLaser) delivered NIR light via a multiple-mode fiber to the surface of the phantom. A single-mode detector fiber connected to an APD module (SPCM-AQ4C, PerkinElmer) and an autocorrelation board (www.correlator.com) was used to collect diffusive light throughout the phantom [9-11]. The distance between the DSCF and DCS probes was 100 mm to prevent interference across the two measurements. The S-D distance was set at 15 mm for both DSCF and DCS measurements. Concurrent DSCF and DCS measurements were performed continuously for 10 seconds at each temperature step (45 °C, 35 °C, 25 °C) with the sampling rates of 4 Hz and 1 Hz, respectively, while the room light was turned off. Flow indices of Intralipid particles measured by the DSCF and DCS were normalized to their respective baselines, yielding relative flow values for comparison.

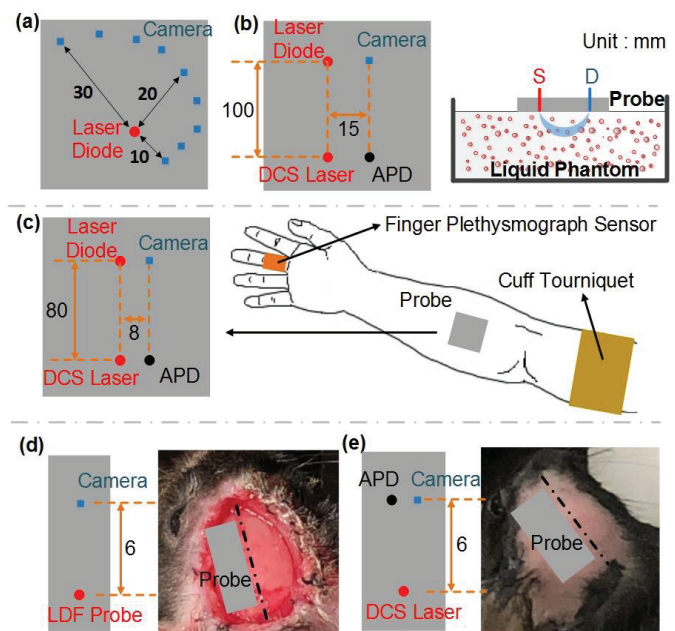


Figure 2: A variety of probes designed for evaluating the performance of DSCF technique. (a) A DSCF probe for testing measurement sensitivity and stability on an Intralipid liquid phantom at different S-D distances. (b) A hybrid probe for concurrent DSCF and DCS measurements of dynamic flow changes of Intralipid particles. (c) A hybrid probe for concurrent DSCF and DCS measurements of forearm blood flow variations during arterial occlusion. (d) A hybrid probe placed on the skull of a mouse head (without scalp) for concurrent DSCF and LDF measurements of CBF variations during TIO. (e) A hybrid probe placed on the head of a mouse (with intact scalp) for concurrent DSCF and DCS measurements of CBF variations during paw electrical stimulations.

Concurrent DSCF and DCS Measurements of Forearm Blood Flow Changes during Cuff Occlusion. Fig. 2c shows a hybrid probe for simultaneous DSCF and DCS measurements of forearm blood flow variations during arterial occlusion. This protocol was approved by the University of Kentucky Institutional Review Board (IRB). A healthy adult extended his arm on a table and the hybrid DSCF/DCS probe was then taped

on the forearm. The S-D distance of 8 mm was used to mimic approximately the largest dimension of a mouse head. A 3-minute arterial cuff occlusion (230 mmHg) paradigm was applied on his upper arm to induce significant blood flow changes in the forearm. Concurrent DSCF and DCS measurements were performed continuously for about 9 minutes (before, during, and after occlusion) with the sampling rates of 4 Hz and 1 Hz, respectively. Blood flow indices measured by DSCF and DCS were normalized to their baselines, respectively, yielding values of relative blood flow (rBF) for comparison.

Additionally, to demonstrate the advantage of faster sampling, the DSCF probe alone was tested on the same forearm at the resting status with a high sampling rate of 20 Hz for 1 minute. Concurrently, a finger plethysmograph sensor (Portapres, FMS) was secured to the index finger for continuous recording of heart beats. The pulsatile blood flow values detected by the DSCF and heart beats were compared for validation.

Continuous Monitoring of CBF Variations in Mice. Fig. 2d shows a hybrid probe designed for concurrent DSCF and LDF measurements of CBF decreases in a mouse during left transient ipsilateral occlusion (TIO). Fig. 2e shows another hybrid probe designed for concurrent DSCF and DCS measurements of CBF increases in another mouse during electrical stimulations between the right forepaw and right hindpaw. The DSCF measurement shared the sources of LDF (Fig. 2d) and DCS (Fig. 2e), respectively. The S-D distance of 6 mm was used in both probes for DSCF measurements, providing a sufficient penetration depth (~ 3 mm) to detect CBF in the mouse cortex. The animal protocols were approved by the University of Kentucky Institutional Animal Care and Use Committee (IACUC).

The mice in both experimental protocols were secured on a stereotaxic frame and anesthetized with 1-2% isoflurane. In the first animal experiment, mouse scalp was retracted to expose the skull. The hybrid DSCF/LDF probe (Fig. 2d) was glued using super glue on the skull above left hemisphere for continuous measurements of CBF before, during, and after TIO. While DSCF data were recorded continuously at a sampling rate of 4 Hz, LDF data were collected by a commercial device (PeriFlux System 5000, PERIMED) visually at only a few time points due to the lack of software for continuous recording. After a baseline measurement for ~ 2 minutes, a silicon-rubber coated 7-0 nylon filament was inserted into internal carotid artery through left common carotid artery and advanced 9 mm beyond bifurcation to induce a TIO for ~ 20 minutes. The suture was then withdrawn allowing reperfusion for 5 minutes. Finally, the cerebral blood supply was completely depleted by traverse cervical clamping under anesthesia. CBF values collected by DSCF and LDF were normalized to their baselines, respectively, yielding values of relative CBF (rCBF) for comparison.

In the second animal experiment, mouse hair was removed but the scalp was kept intact. The hybrid DSCF/DCS probe (Fig. 2e) was glued using super glue on the head of left hemisphere for continuous measurements of CBF during

before, during and after right paw electrical stimulations. A pair of electrodes [22] (Theratouch 4.7, Rich-Mar) were put under the right forepaw and right hindpaw respectively to generate a pulsed square-wave electrical current at 5 Hz. Prior to the experiment, the driving current to the electrodes was gradually increased and initial jitter was observed at 4 mA. Because the animal could adapt the stimulation quickly (within a few seconds), the current was increased continuously from 4 mA to 16 mA with incremental of 4 mA to keep sufficient stimulation strength. The stimulation at each step lasted for ~ 1 minute. Concurrent DSCF and DCS measurements were performed continuously for about 10 minutes (before, during, and after stimulations) with the sampling rates of 4 Hz and 1 Hz, respectively. CBF values collected by DSCF and DCS were normalized to their baselines, respectively, yielding values of rCBF for comparison.

III. RESULTS

A. Phantom Measurement Results

Fig. 3 shows the first phantom results in testing measurement sensitivity and stability at different S-D distances, using a DSCF probe as shown in Fig. 2a. The detected light intensity (digital counts) decreased with the increase of S-D distance, leading to the decrease of SNR (Fig. 3a). When the S-D distances were larger than 15 mm, SNR decreased largely (SNR < 4), associated with instable/inconstant flow indices detected (Fig. 3b). Note that the Intralipid particle flow indices measured at different S-D distances should be constant when the phantom temperature (i.e., room temperature) kept constant [21]. Based on the results, the S-D distance to obtain stable flow measurements with the present DSCF device was determined to be less than 15 mm.

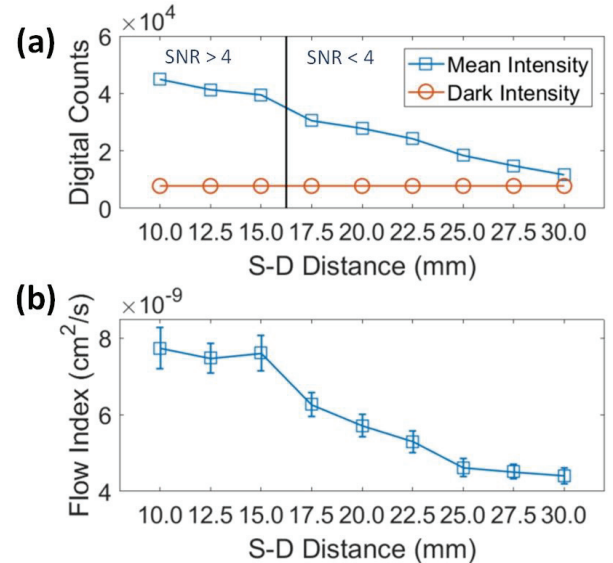


Figure 3: Phantom test results measured by a DSCF probe with different S-D distances, as shown in Fig. 2a. (a) Averaged digital counts (light intensity) versus the dark-noise counts detected by the NanEye 2D camera at different S-D distances. (b) Flow indices (means \pm standard deviations) measured at different S-D distances. The error bar at each S-D distance indicates the flow variation over a measurement period of 10 seconds.

Fig. 4 shows the second phantom results in validating DSCF measurements of dynamic flow changes of Intralipid particles

against DCS, using a hybrid probe with the S-D distance of 15 mm, as shown in **Fig. 2b**. As expected, Intralipid particle flow increased with the increase of the phantom temperature (**Fig. 4a**). The percentage flow changes measured concurrently by the two techniques were significantly correlated ($R^2 = 0.95$, $p < 10^{-5}$), as shown in **Fig. 4b**.

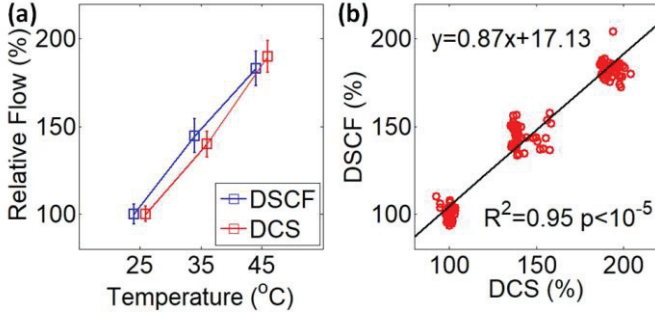


Figure 4: Phantom test results measured by a hybrid DSCF/DCS probe with a fixed S-D distance of 15 mm, as shown in Fig. 2b. (a) Relative flow values (means \pm standard deviations) measured at different temperatures of the liquid phantom. The error bar at each temperature step indicates the flow variation over a measurement period of 10 seconds. (b) Regression correlation between the DSCF and DCS measurements of flow indices at different temperatures.

B. Human Forearm Blood Flow Responses to Cuff Occlusion

Fig. 5 shows the *in vivo* test results on a human forearm, using a hybrid DSCF/DCS probe as shown in **Fig. 2c**. The sampling rate for the DSCF measurement was 4 Hz. The time-course responses of rBF in the forearm before, during, and after cuff occlusion met the expectation of physiological changes due to the occlusion (**Fig. 5a**). A significant correlation between the DSCF and DCS measurements was observed ($R^2 = 0.94$, $p < 10^{-5}$), as shown in **Fig. 5b**. It should be noted that the subject did not feel any heat accumulation on his forearm underneath the hybrid probe over the measurement period of 9 minutes.

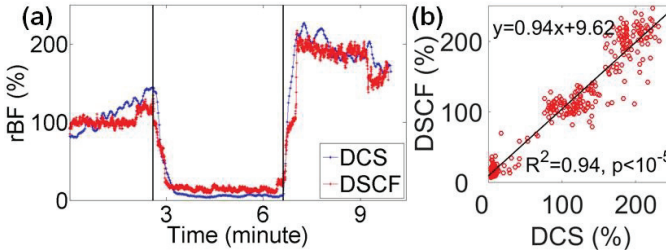


Figure 5: *In vivo* test results on a human forearm during cuff occlusion measured by a hybrid DSCF/DCS probe, as shown in Fig. 2c. (a) Time-course changes of rBF before, during, and after cuff occlusion (b) Regression correlation between the DSCF and DCS measurements of forearm rBF.

Fig. 6 shows the *in vivo* test results in the same forearm at resting status, measured by the DSCF probe alone (**Fig. 2c**) using a higher sampling rate of 20 Hz. The pulsatile blood flow was clearly observed (**Fig. 6a**). The average peak frequency of the pulsatile blood flow was ~ 1.3 Hz (**Fig. 6b**), which agreed with that of ~ 1.2 Hz recorded by the finger plethysmograph sensor.

C. CBF Responses in Mice during TIO and Paw Electrical Stimulations

Fig. 7a shows rCBF variations in a mouse before, during, and after TIO, measured by a hybrid DSCF/LDF probe (**Fig.**

2d). TIO created a dramatic decrease in rCBF, which could be detected by both DSCF and LDF devices (**Fig. 7a**). A significant correlation was observed between the DSCF and LDF measurements ($R^2 = 1.00$, $p < 10^{-5}$), as shown in **Fig. 7b**.

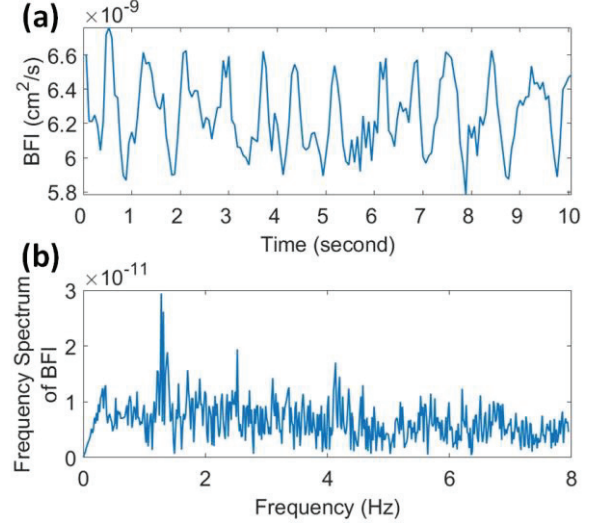


Figure 6: *In vivo* test results on the same forearm at resting status measured by the DSCF probe (Fig. 2c) at a high sampling rate of 20 Hz. (a) The pulsatile blood flow over a zoom-in short period of 10 seconds. (b) The frequency spectrum of resting blood flow indices over a measurement period of 1 minute.

Fig. 8a shows rCBF variations in another mouse before, during, and after paw electrical stimulations, measured by the hybrid DSCF/DCS probe (**Fig. 2e**). The electrical stimulations induced dramatic increases in rCBF, which could be detected by both DSCF and DCS techniques (**Fig. 8a**). A significant correlation was observed between the DSCF and DCS measurements ($R^2 = 0.80$, $p < 10^{-5}$), as shown in **Fig. 8b**.

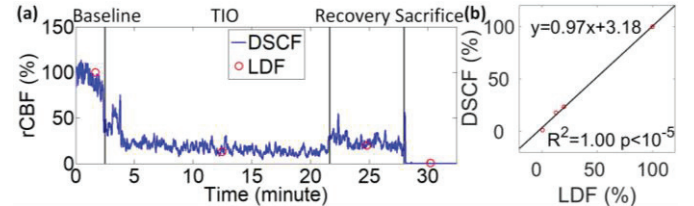


Figure 7: *In vivo* test results in a mouse measured by gluing a hybrid DSCF/LDF probe on the skull (without scalp), as shown in Fig. 2d. (a) Time-course changes in rCBF before, during and after TIO. (b) Regression correlation between the DSCF and LDF measurements of rCBF.

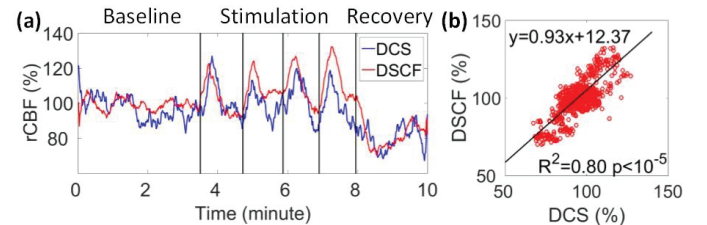


Figure 8: *In vivo* test results in a mouse measured by gluing a hybrid DSCF/DCS probe on the head (with intact scalp), as shown in Fig. 2e. (a) Time-course changes in rCBF before, during and after paw electrical stimulations. (b) Regression correlation between the DSCF and DCS measurements of rCBF.

IV. DISCUSSION AND CONCLUSIONS

We have designed a novel DSCF system including a small fiberless optical probe, which can be installed on the small

mouse head for continuous CBF monitoring (**Fig. 1**). The miniaturized DSCF probe consists of a small laser diode and an ultra-small CMOS camera, which leverages advances made previously from our DSCF prototype implementation [17]. The benefits of contact, fiberless, and reflectance measurement frameworks are retained among both DSCF systems. These benefits result in a small and cost-effective instrumentation for a flexible reflectance measurement to detect blood flow variations in relatively deep tissues. More importantly, the DSCF naturally transmits photovoltaic conversion process to the probe, which makes the signal transition between the probe and a control unit all electric. This advantage enables the DSCF to avoid any signal transition fibers (i.e., fiberless), while those optical fibers are usually too rigid yet fragile to constrain the subject moment. For example, the diffuse speckle contrast analysis (DSCA) [23-25] method uses optical fibers to deliver laser light and guide the detection of camera sensor. Moreover, both DSCA and speckle contrast optical spectroscopy (SCOS) [19, 26] techniques use large cameras working in noncontact manner with or without shielding tubes. As a result, their applications as wearable sensors in freely moving subjects, especially small animals, are constrained.

The improved DSCF system reported in this paper also achieves several unique features over its predecessors [17]. The innovation exclusive to the improved DSCF is minimizing and compacting the probe by means of replacing the large CCD sensor (CMLN-13S2M-CS, Point Grey) with an ultra-small CMOS camera (NanEye 2D, Awaiba). This NanEye 2D camera features in a super tiny volume ($\sim 1 \times 1 \text{ mm}^2$), allowing the DSCF probe to be extremely compact (**Fig. 1a**), compared to the CCD sensor ($\sim 40 \times 40 \text{ mm}^2$) [17]. Also, in contrast to the large power consumption of $\sim 2 \text{ W}$ by the CCD, the power of the NanEye 2D camera is only $\sim 4 \text{ mW}$, suggesting ignorable amount of heat in long-term measurements. The small lens assembled in front of the NanEye 2D camera sensor does not increase the diameter of the camera, but provides a slight focal distance ($\sim 3 \text{ mm}$) from the target surface. In fact, this slight distance provides the protection to the surface tissue (skin) against burn injury from potential heat accumulation.

In a very limited space such as a mouse head, the tiny NanEye camera allows for a high-density sampling (250×250 pixels). The multitudinous pixel grid detection element greatly increases the available pixel windows, thereby enhancing SNR by averaging multiple pixel windows. In addition, the pixel size of $3 \times 3 \mu\text{m}^2$ on our CMOS camera is smaller than that on the CCD camera used previously ($3.75 \times 3.75 \mu\text{m}^2$) [17]. According to Nyquist sampling rule [6], when the wavelength and optical magnification are fixed, smaller pixel size allows to use smaller F number passing more photons to enhance the SNR. Moreover, the high temporal sampling rate (up to 50 Hz) provides another dimension for data process improvement. By averaging flow data from multiple temporal frames, higher SNR can be achieved (**Fig. 5**). Without averaging, on the other hand, fast flow variations can be captured to reveal the pulsatile nature of blood flow (**Fig. 6**). These high spatial-temporal sampling features avoid the situation of using numerous

expensive APDs at slow sampling rate and fiber connections in conventional DCS techniques [9-11].

The improvement in source focuses on a custom-designed power supply with an active feedback circuit. The internal photodiode integrated inside the laser diode package is used to instantly detect the light intensity variation and provide current feedback to actively stabilize the output power (**Fig. 1d**). Also, an adjustment of the full scale photodiode current is provided in order to compensate for the differences in the photodiode currents between different laser diodes for ease of changing the laser source. More importantly, the circuit is controlled by a virtual interface which significantly reduces the space occupied, making the whole system more portable and increasing its potential to be wearable.

It becomes apparent that the major innovation/advantage of the current DSCF over its progenitors is the unique compact and comfort probe with smaller size and less power consumption. Previous DSCF probe with the high-power CCD camera (2 W) has to affiliate heat sinks and run a fan to sustain a normal measurement [17]. However, these addenda enlarge the probe volume and cause more wire connections, thus significantly restrict the application of the technology. By contrast, the current compact probe with small-power CMOS camera (4 mW) can be used for continuous monitoring of blood flow variations in a variety of biological tissues (**Figs 5-8**). The laser diode output power (10 mW) is also within the allowable range of American National Standards Institute (ANSI) for skin protection [27]. As a result, the subject did not feel any heat or burning on the skin even when the DSCF was running at the maximum sampling rate of 55 Hz for 1 hour.

The new DSCF system was characterized using tissue-simulating phantoms, firstly with a constant flow index of Intralipid particles to determine the effective S-D distance range (up to 15 mm, **Fig. 3**) and then with a maximal effective S-D distance (15 mm) to validate the measurement accuracy of dynamic flow changes (**Fig. 4**). Apparently, SNR dropped with the decrease of light intensity detected, especially when the S-D distance was beyond 15 mm. Meanwhile, flow value also dropped dramatically at the S-D distance greater than 15 mm. This trend is similar to our previous findings in tissue phantom tests using a noncontact speckle contrast diffuse correlation tomography system for 3D imaging of blood flow distributions [21], although the effective S-D distance ranges are slightly different due to the difference in camera sensitivities. This largest effective S-D distance (15 mm) is the same as that of our previous DSCF prototype [17]. Moreover, the consistent results between the concurrent DSCF and DCS measurements using this distance (15 mm) in the dynamic liquid phantom further verifies the accuracy of DSCF technique for capturing dynamic flow changes in relatively deep tissues ($\sim 8 \text{ mm}$ depth). This depth is generally sufficient for detecting CBF in the cortices of rodents and newborn infants.

The DSCF device was then tested for *in vivo* monitoring of blood flow changes in a human forearm during cuff occlusion. The forearm has sufficient space to install multiple probes with flexible S-D distances for comparison and the cuff occlusion can be easily applied on the upper arm to create forearm blood

flow variations. As expected, the well-known ischemic (during occlusion) and hyperemic responses (after reperfusion) can be clearly revealed by both DSCF and DCS techniques (Fig. 5). The fast sampling test on the resting forearm at 20 Hz demonstrates the capability of DSCF for detecting the pulsatile blood flow, generated by heart beats (Fig. 6). This high sampling may be crucial for capturing rapid hemodynamic responses, for example, to fast cortical neuronal activities.

Finally, the *in vivo* applications of small DSCF probes on mouse heads demonstrated successes in continuous monitoring of CBF decreases induced by TIO (Fig. 7) and increases induced by paw electrical stimulations (Fig. 8a), respectively. The DSCF measurement results were validated against standard techniques including LDF and DCS. Note that these measurements were performed on the mouse head under two different conditions. i.e., without (Fig. 7) or with (Fig. 8) the scalp. While it is not surprising that the penetration depth of ~3 mm (with a S-D distance of 6 mm) can detect cortex CBF even with the scalp, this flexibility makes it possible for DSCF to work as a wearable sensor for fully noninvasive measurements of CBF in mice.

We noticed that there were insignificant discrepancies among the results from concurrent measurements using different technologies including DSCF, LDF, and DCS (Figs. 4-8). These are likely due to the heterogeneities of tissue hemodynamic responses measured by different probes in different tissue volumes and locations (Fig. 2c-2e). For *in vivo* measurements in human forearm with occlusion (Fig. 5) and mouse brain with paw electrical stimulation (Fig. 8), blood flow did not completely recover to its baseline value at the end of our measurements. This does not affect our comparison results as blood flow was measured concurrently by the two methods (i.e., DSCF and DCS). However, rBF/rCBF measurements should be performed longer in the future to track a fully cerebral recovery. Absolute BFI may be obtained from multiple K measurements at multiple S-D distances or with multiple exposure times to eliminate the influence of an unknown coherence factor β in the Siegert relation [19]. The present study only reported the relative change of BFI, normalized by its baseline (i.e., rBF or rCBF). The β was eliminated by the normalization assuming it is constant. This assumption is generally correct for continuous measurement with no change in optical setup and most of previous studies with DCS reported only relatively changes of tissue blood flow [4, 8, 9, 14, 16, 17, 22, 28-30]. Nonetheless, we will explore absolute BFI measurements in the future by using either multiple cameras placed at different distances from the source or a single camera with multiple exposure times. In addition, the sample size for each experimental protocol was only one in this study since our focus was on the comparison of DSCF with other standards (i.e., LDF and DCS) rather than physiological investigation. We will include more subjects in the future to further verify the measurement accuracy and reproducibility of DSCF and to investigate physiological insights.

Our next step would be adapting the DSCF technique as a wearable sensor for continuous monitoring of CBF variations in freely moving conscious rodents (mice and rats). One challenge is how to design and install a wearable DSCF probe

on the head without significantly interrupting subject's daily activities. Another issue is how to eliminate or reduce motion artifacts resulting from subject's abrupt movement. One option is to learn from the design of a commercial animal cage for electroencephalography (EEG) measurements in freely moving rodents, which allows for the installation of multiple biosensors on rodent's head [31]. Similar to the EEG measurement configuration, the electrical wires used for DSCF measurements can be attached to a low-torque commutator on the top of the cage to allow the animal to move freely and avoid wire twisting. A video camera can be mounted on top of the cage to continuously monitor animal's activities so as to evaluate and reduce the potential impact of motion influences on DSCF measurements. We may also explore the adaption of wearable DSCF technique for continuous cerebral monitoring of critically ill infants who are at high risk for developing neurological morbidities.

In conclusion, the DSCF system is a novel noninvasive optical technology allowing for wearable, fast, continuous, and cost-effective monitoring of CBF in mice. The flexible S-D distance configuration has been shown adaptable to multiple applications as exemplified by the experiments in tissue-simulating phantoms, human forearms, and mouse brains. The flow monitoring capability was calibrated on tissue-simulating phantoms with known optical properties. The applicable viability of the system was proven in quantifying human forearm flow variations at flexible sampling rates. The DSCF system was finally validated for detecting increases and decreases of CBF in mice against the established technologies. This study demonstrates a solid step towards developing a wearable sensor for continuous and longitudinal monitoring of CBF variations in freely moving subjects such as mice, rats, and newborn infants.

REFERENCES

- [1] F. Pizza, M. Biallas, U. Kallweit, M. Wolf, and C. L. Bassetti, "Cerebral hemodynamic changes in stroke during sleep-disordered breathing," *Stroke*, vol. 43, pp. 1951-3, Jul 2012.
- [2] B. J. Saab, A. J. B. MacLean, M. Kanisek, A. A. Zurek, L. J. Martin, J. C. Roder, *et al.*, "Short-term Memory Impairment after Isoflurane in Mice Is Prevented by the $\alpha 5$ γ -Aminobutyric Acid Type A Receptor Inverse Agonist L-655,708," *Anesthesiology*, vol. 113, pp. 1061-1071, 2010.
- [3] N. M. Bornstein, A. Y. Gur, P. Fainshtein, and A. D. Korczyn, "Stroke during sleep: epidemiological and clinical features," *Cerebrovasc Dis*, vol. 9, pp. 320-2, Nov-Dec 1999.
- [4] Y. Shang, L. Chen, M. Toborek, and G. Yu, "Diffuse optical monitoring of repeated cerebral ischemia in mice," *Optics Express*, vol. 19, pp. 20301-20315, Oct 10 2011.
- [5] S. Ansari, H. Azari, D. J. McConnell, A. Afzal, and J. Mocco, "Intraluminal middle cerebral artery occlusion (MCAO) model for ischemic stroke with laser doppler flowmetry guidance in mice," *Journal of Visualized Experiments*, May 8 2011.
- [6] D. A. Boas and A. K. Dunn, "Laser speckle contrast imaging in biomedical optics," *Journal of Biomedical Optics*, vol. 15, p. 011109, Jan-Feb 2010.
- [7] A. K. Dunn, "Laser Speckle Contrast Imaging of Cerebral Blood Flow," *Annals of Biomedical Engineering*, vol. 40, pp. 367-377, Feb 2012.
- [8] R. Cheng, Y. Shang, D. Hayes, S. P. Saha, and G. Yu, "Noninvasive optical evaluation of spontaneous low frequency oscillations in cerebral hemodynamics," *Neuroimage*, vol. 62, pp. 1445-1454, Sep 2012.
- [9] Y. Shang, Y. Zhao, R. Cheng, L. Dong, D. Irwin, and G. Yu, "Portable optical tissue flow oximeter based on diffuse correlation spectroscopy," *Optics Letters*, vol. 34, pp. 3556-3558, Nov 15 2009.

- [10] C. Huang, J. P. Radabaugh, R. K. Aouad, Y. Lin, T. J. Gal, A. B. Patel, *et al.*, "Noncontact diffuse optical assessment of blood flow changes in head and neck free tissue transfer flaps," *Journal of Biomedical Optics*, vol. 20, p. 075008, 2015.
- [11] C. Huang, Y. Lin, L. He, D. Irwin, M. M. Szabunio, and G. Yu, "Alignment of sources and detectors on breast surface for noncontact diffuse correlation tomography of breast tumors," *Applied Optics*, vol. 54, pp. 8808-8816, 2015/10/10 2015.
- [12] Y. Lin, C. Huang, D. Irwin, L. He, Y. Shang, and G. Yu, "Three-dimensional flow contrast imaging of deep tissue using noncontact diffuse correlation tomography," *Applied Physics Letters*, vol. 104, p. 121103, Mar 24 2014.
- [13] D. A. Boas, L. E. Campbell, and A. G. Yodh, "Scattering and Imaging with Diffusing Temporal Field Correlations," *Physical Review Letters*, vol. 75, pp. 1855-1858, Aug 28 1995.
- [14] T. Durduran, C. A. Zhou, E. M. Buckley, M. N. Kim, G. Yu, R. Choe, *et al.*, "Optical measurement of cerebral hemodynamics and oxygen metabolism in neonates with congenital heart defects," *Journal of Biomedical Optics*, vol. 15, May-Jun 2010.
- [15] R. Cheng, Y. Shang, S. Q. Wang, J. M. Evans, A. Rayapati, D. C. Randall, *et al.*, "Near-infrared diffuse optical monitoring of cerebral blood flow and oxygenation for the prediction of vasovagal syncope," *Journal of Biomedical Optics*, vol. 19, p. 017001, Jan 2014.
- [16] L. Chen, Y. Shang, E. Sipos, K. E. Saatman, G. Yu, and M. Toborek, "Novel experimental model for repeated forebrain ischemia-reperfusion," *Journal of Experimental Stroke & Translational Medicine*, vol. 5, pp. 1-10, 2012.
- [17] C. Huang, M. Seong, J. P. Morgan, S. Mazdeyasna, J. G. Kim, J. T. Hastings, *et al.*, "Low-cost compact diffuse speckle contrast flowmeter using small laser diode and bare charge-coupled-device," *Journal of Biomedical Optics*, vol. 21, pp. 080501-080501, 2016.
- [18] G. Yu, C. Huang, and J. T. Hastings, "Compact low-cost fiberless diffuse speckle contrast flow-oximeter," United States Patent Application, #15655988, 2016.
- [19] C. P. Valdes, H. M. Varma, A. K. Kristoffersen, T. Dragojevic, J. P. Culver, and T. Durduran, "Speckle contrast optical spectroscopy, a non-invasive, diffuse optical method for measuring microvascular blood flow in tissue," *Biomed Opt Express*, vol. 5, pp. 2769-84, Aug 1 2014.
- [20] C. Huang, D. Irwin, Y. Lin, Y. Shang, L. He, W. Kong, *et al.*, "Speckle contrast diffuse correlation tomography of complex turbid medium flow," *Medical Physics*, vol. 42, pp. 4000-4006, 2015.
- [21] C. Huang, D. Irwin, M. Zhao, Y. Shang, N. Agochukwu, L. Wong, *et al.*, "Noncontact 3-dimensional Speckle Contrast Diffuse Correlation Tomography of Tissue Blood Flow Distribution," *IEEE Transactions on Medical Imaging*, vol. 36, pp. 2068-2076, 2017.
- [22] Y. Shang, Y. Lin, B. A. Henry, R. Cheng, C. Huang, L. Chen, *et al.*, "Noninvasive evaluation of electrical stimulation impacts on muscle hemodynamics via integrating diffuse optical spectroscopies with muscle stimulator," *J Biomed Opt*, vol. 18, p. 105002, Oct 2013.
- [23] R. Bi, J. Dong, and K. Lee, "Deep tissue flowmetry based on diffuse speckle contrast analysis," *Optics letters*, vol. 38, pp. 1401-3, May 1 2013.
- [24] M. Seong, Z. Phillips, P. M. Mai, C. Yeo, C. Song, K. Lee, *et al.*, "Simultaneous blood flow and blood oxygenation measurements using a combination of diffuse speckle contrast analysis and near-infrared spectroscopy," *Journal of biomedical optics*, vol. 21, p. 27001, Feb 1 2016.
- [25] R. Bi, J. Dong, and K. Lee, "Multi-channel deep tissue flowmetry based on temporal diffuse speckle contrast analysis," *Opt Express*, vol. 21, pp. 22854-22861, Sep 23 2013.
- [26] T. Dragojević, J. L. Hollmann, D. Tamborini, D. Portaluppi, M. Buttafava, J. P. Culver, *et al.*, "Compact, multi-exposure speckle contrast optical spectroscopy (SCOS) device for measuring deep tissue blood flow," *Biomedical Optics Express*, vol. 9, pp. 322-334, 2018/01/01 2018.
- [27] *Laser Safety Manual: UCSB Environmental Health & Safety.*
- [28] C. Zhou, S. A. Eucker, T. Durduran, G. Yu, J. Ralston, S. H. Friess, *et al.*, "Diffuse optical monitoring of hemodynamic changes in piglet brain with closed head injury," *Journal of Biomedical Optics*, vol. 14, May-Jun 2009.
- [29] C. Cheung, J. P. Culver, K. Takahashi, J. H. Greenberg, and A. G. Yodh, "In vivo cerebrovascular measurement combining diffuse near-infrared absorption and correlation spectroscopies," *Physics in Medicine and Biology*, vol. 46, pp. 2053-2065, Aug 2001.
- [30] N. B. Agochukwu, C. Huang, M. Zhao, A. A. Bahrani, L. Chen, P. McGrath, *et al.*, "A Novel Noncontact Diffuse Correlation Spectroscopy Device for Assessing Blood Flow in Mastectomy Skin Flaps: A Prospective Study in Patients Undergoing Prosthesis-Based Reconstruction," *Plast Reconstr Surg*, vol. 140, pp. 26-31, Jul 2017.
- [31] W. C. Clegern, M. E. Moore, M. A. Schmidt, and J. Wisor, "Simultaneous electroencephalography, real-time measurement of lactate concentration and optogenetic manipulation of neuronal activity in the rodent cerebral cortex," *Journal of Visualized Experiments*, p. e4328, Dec 19 2012.

Chong Huang received his Ph.D. degree in Optical Engineering in 2011. He is currently a research scientist in the Department of Biomedical Engineering at the University of Kentucky. His research focuses on the development of diffuse optical technologies for noninvasive assessment of microvasculature hemodynamics in biological tissues.

Yutong Gu is an undergraduate at the University of Southern California with a major of Electrical Engineering. He conducted research for the Department of Biomedical Engineering at the University of Kentucky. He is currently conducting research to develop intelligent robotics.

Jing Chen received her Ph.D. degree in Computer Science in 2016. Her research focuses on human-computer interaction, emotion recognition based on human physiological signals, and data fusion.

Ahmed A. Bahrani received M.Sc. degree from Medical Engineering in 2006. He is now a Ph.D. candidate in the Department of Biomedical Engineering at the University of Kentucky. His research interest includes quantification and analysis of cerebral blood flow using near-infrared diffuse correlation spectroscopy.

Elie G. Abu Jawdeh is an Assistant Professor of Pediatrics at University of Kentucky College of Medicine. His research focuses on predictors and consequences of intermittent hypoxemia (IH) in preterm infants.

Henrietta S. Bada is a Professor of Pediatrics at University of Kentucky College of Medicine and Vice Chair for Academic Affairs at the Department of Pediatrics. Her current interests also include management of neonatal abstinence syndrome and long term developmental follow up.

Kathryn Saatman is a professor of the Department of Physiology and Spinal Cord and Brain Injury Research Center at the University of Kentucky. She is leading the research team in Traumatic Brain Injury and has in-depth experience with qualitative and quantitative measures of brain injury and animal behavioral tests.

Guoqiang Yu is a professor of the Department of Biomedical Engineering at the University of Kentucky. He is the director of bio-photonics laboratory and leading a research group to develop various near-infrared diffuse spectroscopy and tomography systems for noninvasive imaging of deep tissue hemodynamics in animals and humans.

Lei Chen is a research assistant professor of the Department of Physiology, Spinal Cord and Brain Injury Research Center at the University of Kentucky. His research focuses on injurious mechanism of and therapies against brain damage after stroke and brain trauma, and innovative noninvasive monitoring of brain repair process.